

A comparison study between the properties of BHBT₂:PC₇₁BM composite nanotubes and its bulk-heterojunction

Muhamad Doris^{1,2*}, Azzuliani Supangat², Teh Chin Hoong², Khaulah Sulaiman² and Rusli Daik³

¹ Department of Electrical Engineering, Universitas Trisakti, Indonesia

² Low Dimensional Materials Research Centre, Department of Physics, University of Malaya, Malaysia

³ School of Chemical Sciences and Food Technology, Faculty of Science and Technology, Universiti Kebangsaan Malaysia, Malaysia

Abstract

In this study, we investigate the morphological, structural, and optical properties of both bulk-heterojunction and composite nanotubes that are composed of thiophene-based small molecules 1,4-bis (2,2'-bithiopen-5-yl)2,5-dihexyloxybenzene (BHBT₂) and fullerene [6,6]-phenyl C₇₁ butyric acid methyl ester (PC₇₁BM). Mix-blended and template-assisted methods were used to fabricate the bulk-heterojunction and the composite nanotubes, respectively. A single material of BHBT₂ thin films and nanotubes fabricated via spin-coating and template-assisted methods, respectively, were also studied. Two different formations between the bulk-heterojunction and the composite nanotubes were compared to elaborate on their advancement in properties. The absorption spectra of the BHBT₂:PC₇₁BM bulk-heterojunction and the composite nanotubes were found to have fallen within the ultraviolet-visible (UV-vis) range. Field emission scanning electron microscope (FESEM) and high-resolution transmission electron microscope (HRTEM) images showed that the carbon-rich of PC₇₁BM, had successfully infiltrated into the BHBT₂ nanotube to form the BHBT₂:PC₇₁BM

* Corresponding author: m.doris@trisakti.ac.id

¹ Department of Electrical Engineering
Universitas Trisakti, Jakarta, 11440, Indonesia

² Low Dimensional Materials Research Centre, Department of Physics
University of Malaya, Kuala Lumpur, 50603, Malaysia

³ School of Chemical Sciences and Food Technology, Faculty of Science and Technology, Universiti Kebangsaan Malaysia, 43600 UKM Bangi, Selangor, Malaysia

composite nanotubes. However, due to the inconsistent uniformed informal distribution of the infiltration, the charge carrier transfer is seen to be better in the bulk-heterojunction rather than in the composite nanotubes.

Keywords: Thiophene, small molecules, alumina template, bulk-heterojunction, composite nanotube

Background

Organic materials have been of interest to many researchers due to their extraordinary properties such as flexibility, abundance of resources, and low production cost. Initially, the organic materials are only used as electric insulator of electronic devices. However, this has changed after the discovery of the metallic behavior of polyacetylene (PA) by Shirakawa et.al [1]. This discovery has lead to the emergence of other conducting organic materials such as polythiophene (Pth), polypyrrole (PPY), polyaniline (PANI), polycarbazole (PCz), polyparaphenylene vinylene (PPV), poly(3,4-ethylene dioxythiophene) (PEDOT), and polyfuran (PF) [2-9] that to date have been used in numerous electronic devices applications. In addition, many other new organic materials have recently been discovered and used in applications involving electronic nanodevices (field effect transistor, light emitting diode) [10, 11], sensors (chemical, gas, optical, biosensor) [12-15], energy storage systems (solar cells, fuel cells, supercapacitors) [16-18], microwave absorption and electromagnetic shielding [19], and biomedical procedures (drug delivery, protein purification, tissue engineering, neural interfaces, actuators) [20-24]. These materials and applications are fabricated based on polymer which have different properties over its small molecules.

The small molecules based materials are promising as they have the properties of viscoelasticity, toughness, crystallinity, and optical when compared to polymer based materials [25-30]. In this study, we examine a novel Thiophene-based small molecules in which the Thiophene is a heterocyclic compound that consists of a five-membered ring that

has properties still seen as reliable and remarkable to date. Furthermore, Thiophene-based small molecules have extraordinary properties that may compete with its polymer in terms of enhancing the efficiency of perovskite-based solar cells and small molecules organic solar cells [28, 31]. Some applications on small molecules organic solar cells [28, 30-32], inorganic-organic hybrid solar cells [33], and field effect transistor [34-36] have been realized from the thiophene-based small molecules. Therefore, intensive studies of thiophene-based small molecules are as crucial as studies of its thiophene-conjugated polymer.

Thiophene-based small molecules, namely 1,4-bis (2,2'-bithiopen-5-yl)2,5-dihexyloxybenzene (BHBT₂) is a pentamer that consists of four thiophene rings and one benzene ring that binds the two hexyl molecules and thiophene. BHBT₂ has a profound solubility particularly in organic solvents such as chloroform, dichloromethane, and tetrahydrofuran. In addition, it is easily purified through column chromatography and recrystallization techniques. The terminal bithiophene groups in a BHBT₂ pentamer are expected to provide good stability and excellent charge transport properties in the pentamer backbone. Therefore, the coupling of dihexyloxy-p-phenylene moiety with terminal bithiophene groups could improve the pi-electron conjugation path in the pentamer backbone without affecting their optical and electrochemical properties [50].

In this work, one of the key explorations of BHBT₂ properties is on its nanostructures. Nanostructures of small molecules such as nanotubes, nanorods, nanowires, and nanoflowers have been commonly fabricated using the template assisted-method [37-41]. **However, study of BHBT₂ small molecules nanostructures upon the template assisted-method have never been examined to date.** The template used is based on alumina oxide material that consists of orderly nanopores to infiltrate a solution, which in turn molds the nanostructured materials into shape. Formation of nanostructures is important to be studied due to its exceptional

properties over the planar structures. For instance, an active material in organic solar cells that is fabricated into nanostructures with the size that corresponds to visible wavelength can enhance the optical performance of the material [42]. In addition, nanostructuring an active material of solar cells into nanorods, nanotubes, and nanowires increases the surface area of the active layer allowing it to absorb more photons that results in higher efficiency [43, 44]. The template assisted-method is a low cost technique to produce nanostructured materials where the properties of the materials can easily be controlled [37, 45, 46]. The types of nanostructures are affected by the parameters of solution that infiltrate into the template's pores. Molecular weight, solution viscosity, solution concentration, infiltration mechanism, and drying process are some of the parameters that influence the formation of nanostructures [39, 40]. Template-assisted method also can be used to fabricate the donor-acceptor system of p-n junction composite nanotubes [47]. Unlike the well-known donor-acceptor system of bulk-heterojunction, the composite nanotubes that are composed of an ordered array of p-n core-shell junctions could accommodate well to the higher carriers mobility. The p-n core-shell junction is widely used in applications such as drug delivery and optoelectronic [48, 49]. As reported previously, a p-n core-shell junction nanowire that was applied to inorganic solar cells have been seen to have improved the efficiency performance of the device [44]. On top of that, the p-n core-shell junction of composite nanotubes could also enhance the charge carrier transfer when compared with its bulk-heterojunction [47].

In this study, the p-n core-shell junction of composite nanotubes has been successfully produced via the template assisted-method. Composite nanotubes of BHBT₂ and fullerene [6,6]-phenyl C₇₁ butyric acid methyl ester (PC₇₁BM) have also been fabricated and characterized. The characterizations are particularly emphasized on the optical, morphological, and structural properties of BHBT₂:PC₇₁BM. The two different formations of bulk-heterojunction and composite nanotubes of BHBT₂:PC₇₁BM are then studied. To the

best of our knowledge, there have been no studies that have investigated the properties of thiophene-based small molecules BHBT₂. Therefore, studies on the p-n BHBT₂:PC₇₁BM properties may provide informative and useful knowledge.

Methods

Thiophene-based small molecules, 1,4-bis (2,2'-bithiophene-5-yl)2,5-dihexyloxybenzene (BHBT₂) were synthesized and used directly as needed. As shown in Figure 1a, BHBT₂ contains a single benzene with four thiophene rings flank the benzene ring on each side. 5 mg of BHBT₂ was dissolved into the 1 ml of chloroform where the solubility limit of BHBT₂ within chloroform is 59 mg ml⁻¹ [50]. A similar concentration of 5 mg/ml was applied to [6,6]-phenyl C₇₁ butyric acid methyl ester (PC₇₁BM), by dissolving it in chloroform. The volume ratio of 1:1 was used to produce the BHBT₂:PC₇₁BM bulk-heterojunction and composite nanotubes. A porous alumina template with 20 nm and 60 μm of pores in diameter and thickness, respectively, was purchased from Whatman Anodisc and was utilized to fabricate the nanostructures. Prior to the infiltration, the templates were cleaned by immersing them in acetone under sonication for 15 min, and then rinsed using deionized water. Three different spin coating rates of 1000, 2000, and 3000 rpm were used in 30 s. Prior to the spin coating process, the templates were first attached onto a glass slide using scotch tape on its right and left sides (Figure 1b). The scotch tape was used to ensure that the template would remain stuck on the glass slide during the spin coating process. Figure 1c shows the infiltrated BHBT₂ after and before the spin coating and dissolution process, respectively.

Figure 2 represents the schematic illustrations of the formation of the BHBT₂ nanotubes and the BHBT₂:PC₇₁BM composite nanotubes. The porous alumina template was first cleaned under sonication of acetone (i). Prior to the spin coating process, 50 μL of BHBT₂ solution was dropped onto the cleaned template, which allowed the solution to infiltrate into the template (ii). To fabricate the BHBT₂:PC₇₁BM composite nanotubes, 50 μL of PC₇₁BM were dropped on top of the infiltrated BHBT₂ followed by the spin coating process (iii). Templates with infiltrated materials were then dried under room temperature.

These templates were stuck upside down on a copper tape (iv) before the dissolution of 6 h in 5 M of sodium hydroxide (NaOH) took place (v). In order to wash the remaining template thoroughly, it was rinsed several times using deionized water. Finally, the obtained nanotubes that remain stuck on the copper tape were ready to be characterized (vi). Schematic illustrations shown in Figure 2 were adapted from the sample preparation set up shown in Figure 3. It can be clearly seen that the infiltrated BHBT₂ presented with a yellow appearance (Figure 3a). The BHBT₂ nanotubes were able to retain their adhesion on the copper tape although the sample was washed for several times (Figure 3b). The BHBT₂:PC₇₁BM composite nanotubes turned brownish due to the infiltration of the PC₇₁BM (Figure 3c). As with the BHBT₂ nanotubes, the BHBT₂:PC₇₁BM composite nanotubes were also be able to remain stuck upside down on the copper tape after several washing (Figure 3d).

Several equipment such as the spin coater model WS-650MZ-23NPP (Laurell Technologies Corp., North Wales, PA, USA), Field Emission Scanning Electron Microscope (FESEM) (Quanta FEG 450), High Resolution Transmission Electron Microscope (HRTEM) (Tecnai G2 FEI), Raman and photoluminescence (PL) spectroscopy (RENISHAW), UV-vis spectroscopy (Shimadzu UV-3101PC) and X-ray Diffraction Spectroscopy (XRD) were used in this study.

Results and discussion

In this study, the properties of single material and composite materials comprised of BHBT₂ (p-type) and fullerene (n-type) are reported. BHBT₂ (1,4-bis (2,2'-bithiophene-5-yl)2,5-dihexyloxybenzene) is a novel small molecule with pentamer [50] and the advantage of high solubility with most solvents. By investigating its optical, morphological and structural properties, new applications on organic electronics devices can be realized to improve the device performance. Based on the X-ray Diffraction (XRD) measurement of BHBT₂ shown in Figure 4a, multiple peaks that represent the BHBT₂ pristine indicate that the BHBT₂ small molecule is a crystalline material [51]. Crystalline materials with periodic structure may provide a light management ability that can outperform the devices, for instance, the enhancement of photon absorption [52-54]. To elaborate on the properties of BHBT₂ small molecules further, incorporation of BHBT₂ and a p-type material of PC₇₁BM is applied. Nanostructuring these materials into p-n composite may enrich knowledge in nano-morphology studies. In addition, the charge transfer between donor and acceptor materials can be better understood and digested when there is more information on the carrier's behaviors. Figure 4b shows the energy diagram of BHBT₂ and PC₇₁BM with HOMO-LUMO of 1.96-4.65 eV and 3.94-5.93 eV, respectively. The HOMO-LUMO of donor-acceptor will enable the exciton (electron-hole) to dissociate at the interface [55].

Optical properties studies

Figure 5a and Figure 5b show the absorption range of BHBT₂ thin films and the nanotubes spin-coated at the different rates of 1000, 2000, and 3000 rpm, respectively. **Increasing the spin coating rate was applied to produce thinner films of the BHBT₂.** A similar pattern of wavelength absorption is shown with the dissimilarity in absorption intensity where **hypochromic effect have occurred in which decreasing the intensity of absorbance as effect**

of less materials that absorb photon. This can be understood that the differences in the thickness of material depends on the spin coating rate in which the thicker layer will absorb more photon. From the UV-vis absorption spectra, BHBT₂ thin films and nanotubes portrayed five significant absorption peaks. No single peak shifting either to left or right side was observed to have taken place, due to the different spin coating rates, apart from the changes in the absorption intensity of BHBT₂ nanotubes, which get higher at 350 nm when compared to its thin films. It was noticed that BHBT₂ favorably absorb photon only in the range of UV and visible light region. Due to its light absorption properties, BHBT₂ may potentially be applied as UV-vis photodetector or as a booster material of active layer in organic photovoltaic applications. Fabricating this material into highly ordered nanostructures may enhance its performance since the charge carrier's transfer mobility can be improved via the highly ordered structures [56, 57]. As shown in Figure 6a, BHBT₂ nanotubes reveal significantly higher absorption intensity in comparison to their thin films [56]. BHBT₂ nanotubes and thin films exhibit four shoulders with their significant peaks occurring at 335, 350, 414, 429, and 461 nm. The longer absorption wavelength of both BHBT₂ nanotubes and thin films are observed at 461 nm of Soret peak (B-band). This condition occurs due to movement of an electron dipole that corresponds to nonbonding-antibonding ($n-\pi^*$) excitation among BHBT₂ molecules. A small part of UV light disclosed at around 320 - 350 nm is attributed to the bonding-antibonding ($\pi-\pi^*$) excitation. Generally, nanostructuring the BHBT₂ either in single material or composite has increased its absorption performance. Incorporating BHBT₂ with PC₇₁BM slightly shifted the intense absorption and rendered the absorption range broader at 320-350 nm and 400-460 nm. As shown in Figure 6b, although the presence of $\pi-\pi^*$ transition was observed in the BHBT₂ bulk-heterojunction, the better absorption was exhibited in the BHBT₂ composite nanotubes.

In an organic material, once a photon bombards onto a donor material, exciton, which is a pair of electron-hole that binds with each other, will be generated. In order to generate a current, this exciton will need to be dissociated by dislodging the electron from its binding energy. One condition that has to be fulfilled is the affinity electron requirement of each donor and acceptor materials. In our study, to investigate the potential application of BHBT₂ into a device, BHBT₂ and electron acceptor of PC₇₁BM were mixed. It should be possible to create a charge transfer phenomena via the HOMO-LUMO configuration of both materials since the electron affinity of the acceptor material is bigger than that of the donor. Charge carriers transfer will only occur when the binding energy of exciton is lower than the electron affinity energy difference between the donor and acceptor materials [58].

The photoluminescence (PL) measurement was carried out to investigate the effectiveness of charge transfer between the donor and acceptor for both the bulk heterojunction and the composite nanotubes. The PL provides information on how well the exciton can reach the donor-acceptor interfaces [59]. Exciton (a pair of electron-hole) that has been generated by the donor material needs to be separated for the current extraction. Recombination of exciton will lead to the emission of radiative photon (radiative recombination) which is shown as intensity in the PL spectra [60]. Excitons that have successfully reached the donor-acceptor interfaces will be dissociated into hole and electron. This phenomenon is indicated by the lower intensity exhibited by the PL peak (quenching) compared to the curve of the radiative recombination which always exhibit the higher intensity. Quenching is attributed to the charge carriers transfer that had occurred between the donor and acceptor, which are carriers produced from the dissociated excitons at the donor-acceptor interfaces [59, 60]. As shown in Figure 7a, the quench phenomenon occurred due to the incorporation of BHBT₂ with PC₇₁BM, which allowed electrons from BHBT₂ to jump to the acceptor material. It is hardly to obtain the photoluminescence results for thin films that

were spin-coated at 1000, 2000, and 3000 rpm at a concentration of 5 mg/ml based on the thickness matter. To solve this hindrance, drop-casting of the solution onto a glass substrate is applied in order to get the feasible films thickness. It is noticed that BHBT₂ thin films has a higher photoluminescence intensity compared to the BHBT₂ bulk-heterojunction and composite nanotubes. Mixing of two materials in the formation of bulk-heterojunction and composite nanotubes has gained almost totally quenching. Figure 7b shows the photoluminescence spectra of BHBT₂ bulk-heterojunction and composite nanotubes. BHBT₂ bulk-heterojunction got slightly quenched compared to its composite nanotubes. Charge transfer between BHBT₂ and PC₇₁BM in the formation of bulk-heterojunction was more effective than the composite nanotubes. Based on the morphology view of bulk-heterojunction, the donor and acceptor will easily agglomerate and mix together in order to allow the electron to reach the donor-acceptor interface. Better quenching of BHBT₂:PC₇₁BM bulk-heterojunction produced results which contradict the results found by other studies [45, 47] where nanostructuring a material gets better quenching than bulk-heterojunctioning. The morphology of BHBT₂:PC₇₁BM composite nanotubes could be responsible for the better quenching of bulk-heterojunction where it could be predicted that most of the BHBT₂:PC₇₁BM composite nanotube interfaces were unevenly constructed.

Structural properties studies

Raman spectroscopy was applied to study the chemical and structural composition of materials. In its application, incident photons that interact with materials may lose or gain energy. The energy difference between the scattered photon and the incident photon is exactly similar to the energy difference in molecular vibration. Therefore, patterns of Raman spectra are generated from the molecular or lattice vibrations within the materials. A low frequency in the Raman shift corresponds to a low energy vibration of atoms which means that heavy atoms are held together with the weak bonds. On the other hand, a high frequency

corresponded to light atoms which were held together with a strong bound [61]. Figure 8a and 8b show the Raman spectra of BHBT₂ thin films versus nanotubes and the Raman spectra of BHBT₂:PC₇₁BM bulk-heterojunction versus composite nanotubes, respectively, with their Raman peaks tabulated in Table 1. Raman peak at 1445 cm⁻¹ shows a slightly different in intensity between BHBT₂ thin films and nanotubes indicating that the thiophenes ring was dominantly stretching in thin film compared to its nanotubes. The occurrence of thiophenes ring stretching supports the existence of BHBT₂ molecular structure with four thiophene rings attached to one benzene ring. However, the incorporation of two materials resulted in shifting around 3 cm⁻¹ to the lower frequency. This shifting could be due to the effect of incidence energy that was divided and served to the two different molecules, which in turn resulted in a decrease in scattered energy [61]. Most of the Raman peaks of BHBT₂ nanotubes shifted to higher frequencies except for the peak at 1564 cm⁻¹ that shifted to lower a frequency for 2 cm⁻¹. However, no CH deformation occurred in BHBT₂ nanotubes. Ring breathing and ring vibration para-substituted benzene were formed from the incorporation of BHBT₂ and PC₇₁BM. These rings were found at 1188 cm⁻¹ and 1227 cm⁻¹, respectively. BHBT₂ composite nanotubes showed shifting to the higher frequencies of 1189 cm⁻¹, and 1231 cm⁻¹. Among the four Raman spectra (BHBT₂ thin films, BHBT₂ nanotubes, BHBT₂:PC₇₁BM bulk heterojunction, and BHBT₂:PC₇₁BM composite nanotubes), BHBT₂ nanotubes and BHBT₂:PC₇₁BM composite nanotubes had somewhat a similar intensity although the highest peak intensity was dominated by BHBT₂ thin films.

Formation of nanostructured composite

BHBT₂ nanotubes were synthesized via the template-assisted method. Figure 9a-c show the FESEM images of BHBT₂ nanotubes obtained from the three different spin coating rates of 1000, 2000, and 3000 rpm. Generally, the nanostructures created bundles of nanotubes by

collapsing their tips with each other instead of growing aligned as a single nanotube. Formation of nanotubes bundles could be due to the presence of attractive forces (van der Waals interactions) between the nanotubes [40]. At spin coating rate of 1000 rpm, the morphology of BHBT₂ nanotubes were produced inconsistently with some of the tubes longer than others. However, with the increase of the spin coating rate to 2000 rpm, the homogeneous growth of BHBT₂ nanotubes was attained. A further increase to 3000 rpm, resulted in a thicker base layer and denser nanotubes. Due to the thicker base layer, the nanotubes bundles become more intricate as the base layer almost covered the nanotubes' structure. Through further investigation, a spin coating rate at 2000 rpm was considered as an optimum parameter for the fabrication of BHBT₂:PC₇₁BM composites.

During the infiltration, the solution that passes through the template nanochannels may experience two possible conditions along the process. The first possible condition is that the solution will spread and wet the nanochannels' wall, which will in turn produce the hollow nanotubes after the template dissolution. The other possible condition is the formation of nanorods, due to the existence of force interactions between the molecules (solution) during infiltration that are stronger than the adhesive force (wall). In this study, the growth mechanism of BHBT₂ nanostructures was rendered by the first possible condition (Figure 10 a-d). Since the optimum spin coating rate is 2000 rpm (BHBT₂ nanotubes), BHBT₂:PC₇₁BM composite nanotubes were then produced at this optimum rate. Observation of hollow structure supported the prediction of wall wetting and force interaction between the wall and the solution. The wall of BHBT₂:PC₇₁BM composite nanotubes were found to be thicker than that of the BHBT₂ nanotubes due to the infiltration of two different materials (BHBT₂ and PC₇₁BM).

Figures 11a and 11b show the HRTEM images of BHBT₂ nanotubes and BHBT₂:PC₇₁BM composite nanotubes, respectively. BHBT₂ nanotubes contain only a single wall of tube whereas BHBT₂:PC₇₁BM composite nanotubes exhibit two different regions. These two different regions corresponded to the PC₇₁BM (inner) and BHBT₂ (outer), respectively. PC₇₁BM was infiltrated into the center of the hollow BHBT₂, which is shown as a darker region. PC₇₁BM of carbon rich materials was successfully infiltrated into the BHBT₂ nanotubes and wetted the inner wall of nanotubes, which led to the formation of p-n junction. If the assumption is that all of the PC₇₁BM had totally infiltrated into the BHBT₂ nanotubes, a more effective charge transfer will take place in composite nanotubes rather than in the bulk-heterojunction. However, based on the morphological images, it was notice that not many PC₇₁BM had been infiltrated into the BHBT₂ nanotubes. In addition to that, the nanotubes were not homogeneously constructed in terms of size. The occurrence of this phenomenon may have been due to the spin coating rate. In the spin coating process, some of the substances may have been swept away, out of the alumina template surface. Ideally, PC₇₁BM substances would have to fully infiltrate the BHBT₂ nanotubes and to have a well-mixed of donor-acceptor interfaces in order to form the homogeneous composite nanotubes. Therefore, the composite nanotubes would provide the more effective way for the charges to be transferred into the acceptor material.

Conclusions

We have successfully synthesized and characterized the properties of 1,4-bis (2,2'-bithiopen-5-yl)2,5-dihexyloxybenzene (BHBT₂) as single material and composites. The comparison study between BHBT₂ thin films, BHBT₂ nanotubes, BHBT₂:PC₇₁BM bulk-heterojunction and BHBT₂:PC₇₁BM composite nanotubes emphasized on their optical, structural and morphological properties. Nanostructuring the BHBT₂ via template-assisted method had been successfully applied to produce nanotubes and composite nanotubes. Better quenching and

improvement of charge carriers' transport was observed in BHBT₂:PC₇₁BM bulk-heterojunction due to the poor interfaces morphology of unevenly constructed BHBT₂:PC₇₁BM composite nanotubes. However, the enhancement of light absorption was observed in BHBT₂ nanotubes and BHBT₂:PC₇₁BM composite nanotubes. PC₇₁BM had been successfully infiltrated into the BHBT₂ nanotubes due to the wetting properties possessed by both materials, although the uniformity of infiltration is poor.

Abbreviations

BHBT₂, 1,4-bis (2,2'-bithiopen-5-yl)2,5-dihexyloxybenzene; FESEM, field emission scanning electron microscopy; HOMO, highest occupied molecular orbital; HRTEM, high resolution transmission electron microscopy; LUMO, lowest unoccupied molecular orbital; NaOH, sodium hydroxide; PA, polyacetylene; PANI, polyaniline; PC₇₁BM, [6,6]-phenyl C₇₁-butyric acid methyl ester; PCz, polycarbazole; PEDOT, poly(3,4-ethylene dioxythiophene); PF, polyfuran; PL, photoluminescence; Pth, polythiophene; PPV, polyparaphenylene vinylene; PPY, polypyrrole; XRD, X-ray Diffraction Spectroscopy

Competing interests

The authors declare that they have no competing interests.

Authors' contributions

MD carried out the experiments, performed the analysis, and drafted the manuscript. AS participated in the design of the study, performed the analysis, and helped draft the manuscript. TCH carried out the experiments, and performed the analysis. KS and RD participated in the design of the study and in the sequence alignment.

Authors' information

MD is a senior lecturer at the Universitas Trisakti. TCH is currently on postdoctoral fellowship at the University of Malaya. AS is the senior lecturer and KS is an associate professor at the Department of Physics, University of Malaya, while RD is a professor at the National University of Malaysia.

Acknowledgements

The authors would like to acknowledge the University of Malaya for the project funding under the University of Malaya High Impact Research Grant UM-MoE (UM.S/625/3/HIR/MoE/SC/26), University Malaya Research Grant (RG283-14AFR), and the Malaysian Ministry of Education for the project funding under the Fundamental Research Grant Scheme (FP002-2013A).

References

1. Shirakawa H, Louis EJ, MacDiarmid AG, Chiang CK, Heeger AJ: **Synthesis of electrically conducting organic polymers: halogen derivatives of polyacetylene, (CH)**. *Journal of the Chemical Society, Chemical Communications* 1977, **16**:578-580.
2. Kirchmeyer S, Reuter K: **Scientific importance, properties and growing applications of poly(3,4-ethylenedioxythiophene)**. *Journal of Materials Chemistry* 2005, **15**(21):2077-2088.
3. Booth MA, Leveneur J, Costa AS, Kennedy J, Travas-Sejdic J: **Tailoring the Conductivity of Polypyrrole Films Using Low-Energy Platinum Ion Implantation**. *The Journal of Physical Chemistry C* 2012, **116**(14):8236-8242.
4. Ćirić-Marjanović G: **Recent advances in polyaniline research: Polymerization mechanisms, structural aspects, properties and applications**. *Synthetic Metals* 2013, **177**(0):1-47.
5. Chen Q, Liu DP, Zhu JH, Han BH: **Mesoporous Conjugated Polycarbazole with High Porosity via Structure Tuning**. *Macromolecules* 2014, **47**(17):5926-5931.
6. Bajpai M, Srivastava R, Dhar R, Tiwari RS, Chand S: **p-Type doping of tetrafluorotetracyanoquinodimethane (F4TCNQ) in poly(para-phenylene vinylene) (PPV) derivative "Super Yellow" (SY)**. *RSC Advances* 2014, **4**(88):47899-47905.
7. Sreeram A, Patel NG, Venkatanarayanan RI, McLaughlin JB, DeLuca SJ, Yuya PA, Krishnan S: **Nanomechanical properties of poly(para-phenylene vinylene) determined using quasi-static and dynamic nanoindentation**. *Polymer Testing* 2014, **37**(0):86-93.
8. Atanasov SE, Losego MD, Gong B, Sachet E, Maria J-P, Williams PS, Parsons GN: **Highly Conductive and Conformal Poly(3,4-ethylenedioxythiophene) (PEDOT) Thin Films via Oxidative Molecular Layer Deposition**. *Chemistry of Materials* 2014, **26**(11):3471-3478.
9. Sheberla D, Patra S, Wijsboom YH, Sharma S, Sheynin Y, Haj-Yahia A-E, Barak AH, Gidron O, Bendikov M: **Conducting polyfurans by electropolymerization of oligofurans**. *Chemical Science* 2015, **6**(1):360-371.
10. Lee SY, Choi GR, Lim H, Lee KM, Lee SK: **Electronic transport characteristics of electrolyte-gated conducting polyaniline nanowire field-effect transistors**. *Applied Physics Letters* 2009, **95**(1):013113.
11. Grimsdale AC, Leok Chan K, Martin RE, Jokisz PG, Holmes AB: **Synthesis of Light-Emitting Conjugated Polymers for Applications in Electroluminescent Devices**. *Chemical Reviews* 2009, **109**(3):897-1091.
12. Rajesh, Ahuja T, Kumar D: **Recent progress in the development of nano-structured conducting polymers/nanocomposites for sensor applications**. *Sensors and Actuators B: Chemical* 2009, **136**(1):275-286.

13. Menegazzo N, Herbert B, Banerji S, Booksh KS: **Discourse on the utilization of polyaniline coatings for surface plasmon resonance sensing of ammonia vapor.** *Talanta* 2011, **85**(3):1369-1375.
14. Michira I, Akinyeye R, Baker P, Iwuoha E: **Synthesis and Characterization of Sulfonated Polyanilines and Application in Construction of a Diazinon Biosensor.** *International Journal of Polymeric Materials and Polymeric Biomaterials* 2011, **60**(7):469-489.
15. Wang X, Shao M, Shao G, Fu Y, Wang S: **Reversible and efficient photocurrent switching of ultra-long polypyrrole nanowires.** *Synthetic Metals* 2009, **159**(3-4):273-276.
16. Fischer FSU, Trefz D, Back J, Kayunkid N, Tornow B, Albrecht S, Yager KG, Singh G, Karim A, Neher D, Brinkmann M, Ludwigs S: **Highly Crystalline Films of PCPDTBT with Branched Side Chains by Solvent Vapor Crystallization: Influence on Opto-Electronic Properties.** *Advanced Materials* 2015, **27**(7):1223-1228.
17. Ma Y, Jiang S, Jian G, Tao H, Yu L, Wang X, Wang X, Zhu J, Hu Z, Chen Y: **CNx nanofibers converted from polypyrrole nanowires as platinum support for methanol oxidation.** *Energy & Environmental Science* 2009, **2**(2):224-229.
18. Chen L, Yuan C, Dou H, Gao B, Chen S, Zhang X: **Synthesis and electrochemical capacitance of core-shell poly (3,4-ethylenedioxythiophene)/poly (sodium 4-styrenesulfonate)-modified multiwalled carbon nanotube nanocomposites.** *Electrochimica Acta* 2009, **54**(8):2335-2341.
19. Saini P, Choudhary V, Singh BP, Mathur RB, Dhawan SK: **Polyaniline-MWCNT nanocomposites for microwave absorption and EMI shielding.** *Materials Chemistry and Physics* 2009, **113**(2-3):919-926.
20. Kim S, Kim J-H, Jeon O, Kwon IC, Park K: **Engineered polymers for advanced drug delivery.** *European Journal of Pharmaceutics and Biopharmaceutics* 2009, **71**(3):420-430.
21. Zhu Y, Li J, Wan M, Jiang L: **Superhydrophobic 3D Microstructures Assembled From 1D Nanofibers of Polyaniline.** *Macromolecular Rapid Communications* 2008, **29**(3):239-243.
22. Srivastava S, Chakraborty A, Salunke R, Roy P: **Development of a Novel Polygalacturonic Acid-Gelatin Blend Scaffold Fabrication and Biocompatibility Studies for Tissue-Engineering Applications.** *International Journal of Polymeric Materials and Polymeric Biomaterials* 2012, **61**(9):679-698.
23. Kang G, Borgens RB, Cho Y: **Well-Ordered Porous Conductive Polypyrrole as a New Platform for Neural Interfaces.** *Langmuir* 2011, **27**(10):6179-6184.
24. Otero TF, Sanchez JJ, Martinez JG: **Biomimetic Dual Sensing-Actuators Based on Conducting Polymers. Galvanostatic Theoretical Model for Actuators Sensing Temperature.** *The Journal of Physical Chemistry B* 2012, **116**(17):5279-5290.
25. Fischer I, Kaeser A, Peters-Gumbs MAM, Schenning APHJ: **Fluorescent π -Conjugated Polymer Dots versus Self-Assembled Small-Molecule Nanoparticles: What's the Difference?.** *Chemistry – A European Journal* 2013, **19**(33):10928-10934.
26. Liu Y, Chen C-C, Hong Z, Gao J, Yang YM, Zhou H, Dou L, Li G, Yang Y: **Solution-processed small-molecule solar cells: breaking the 10% power conversion efficiency.** *Nature Scientific Reports* 2013, **3**:3356.
27. Zhang Q, Kan B, Liu F, Long G, Wan X, Chen X, Zuo Y, Ni W, Zhang H, Li M, Hu Z, Huang F, Cao Y, Liang Z, Zhang M, Russell TP, Chen Y: **Small-molecule solar cells with efficiency over 9%.** *Nat Photon* 2015, **9**(1):35-41.
28. Li H, Fu K, Boix PP, Wong LH, Hagfeldt A, Grätzel M, Mhaisalkar SG, Grimsdale AC: **Hole-Transporting Small Molecules Based on Thiophene Cores for High Efficiency Perovskite Solar Cells.** *ChemSusChem* 2014, **7**(12):3420-3425.
29. Mishra A, Bäuerle P: **Small Molecule Organic Semiconductors on the Move: Promises for Future Solar Energy Technology.** *Angewandte Chemie International Edition* 2012, **51**(9):2020-2067.

30. Zhou J, Wan X, Liu Y, Zuo Y, Li Z, He G, Long G, Ni W, Li C, Su X, Chen Y: **Small Molecules Based on Benzo[1,2-b:4,5-b']dithiophene Unit for High-Performance Solution-Processed Organic Solar Cells.** *Journal of the American Chemical Society* 2012, **134**(39):16345-16351.
31. Malyskyi V, Simon JJ, Patrone L, Raimundo JM: **Thiophene-based push-pull chromophores for small molecule organic solar cells (SMOSCs).** *RSC Advances* 2015, **5**(1):354-397.
32. Montcada NF, Pelado B, Viterisi A, Alberio J, Coro J, Cruz Pdl, Langa F, Palomares E: **High open circuit voltage in efficient thiophene-based small molecule solution processed organic solar cells.** *Organic Electronics* 2013, **14**(11):2826-2832.
33. Freitas FS, Clifford JN, Palomares E, Nogueira AF: **Tailoring the interface using thiophene small molecules in TiO₂/P3HT hybrid solar cells.** *Physical Chemistry Chemical Physics* 2012, **14**(34):11990-11993.
34. Park JI, Chung JW, Kim JY, Lee J, Jung JY, Koo B, Lee BL, Lee SW, Jin YW, Lee SY: **Dibenzothiopheno[6,5-b:6',5'-f]thieno[3,2-b]thiophene (DBTTT): High-Performance Small-Molecule Organic Semiconductor for Field-Effect Transistors.** *Journal of the American Chemical Society* 2015. doi:10.1021/jacs.5b01108
35. Sun J-P, Hendsbee AD, Eftaiha AaF, Macaulay C, Rutledge LR, Welch GC, Hill IG: **Phthalimide-thiophene-based conjugated organic small molecules with high electron mobility.** *Journal of Materials Chemistry C* 2014, **2**(14):2612-2621.
36. Wang C, Zang Y, Qin Y, Zhang Q, Sun Y, Di C-a, Xu W, Zhu D: **Thieno[3,2-b]thiophene-Diketopyrrolopyrrole-Based Quinoidal Small Molecules: Synthesis, Characterization, Redox Behavior, and n-Channel Organic Field-Effect Transistors.** *Chemistry – A European Journal* 2014, **20**(42):13755-13761.
37. Al-Kaysi RO, Ghaddar TH, Guirado G: **Fabrication of one-dimensional organic nanostructures using anodic aluminum oxide templates.** *Journal of Nanomaterials* 2009, Article ID 436375
38. Hu J, Shirai Y, Han L, Wakayama Y: **Template method for fabricating interdigitate p-n heterojunction for organic solar cell.** *Nanoscale Res Lett* 2012, **7**(1):1-5.
39. Fakir MS, Supangat A, Sulaiman K: **Templated growth of PFO-DBT nanorod bundles by spin coating: effect of spin coating rate on the morphological, structural, and optical properties.** *Nanoscale Res Lett* 2014, **9**(1):1-7.
40. Bakar NA, Supangat A, Sulaiman K: **Elaboration of PCDTBT nanorods and nanoflowers for augmented morphological and optical properties.** *Materials Letters* 2014, **131**:27-30.
41. Jung WS, Do YH, Kang MG, Kang CY: **Energy harvester using PZT nanotubes fabricated by template-assisted method.** *Current Applied Physics* 2013, **13**, Supplement 2 (0):S131-S134.
42. Edman Jonsson G, Fredriksson H, Sellappan R, Chakarov D: **Nanostructures for Enhanced Light Absorption in Solar Energy Devices.** *International Journal of Photoenergy* 2011, Article ID 939807.
43. Yu K, Chen J: **Enhancing solar cell efficiencies through 1-D nanostructures.** *Nanoscale Res Lett* 2009, **4**(1):1-10
44. Wang S, Yan X, Zhang X, Li J, Ren X: **Axially connected nanowire core-shell pn junctions: a composite structure for high-efficiency solar cells.** *Nanoscale Res Lett* 2015, **10**(1):1-7.
45. Supangat A, Kamarundzaman A, Bakar NA, Sulaiman K, Zulfiqar H: **P3HT: VOPcPhO composite nanorods arrays fabricated via template-assisted method: Enhancement on the structural and optical properties.** *Materials Letters* 2014, **118**:103-106.
46. Kamarundzaman A, Fakir MS, Supangat A, Sulaiman K, Zulfiqar H: **Morphological and optical properties of hierarchical tubular VOPcPhO nanoflowers.** *Materials Letters* 2013, **111**(0):13-16.
47. Makinudin AHA, Fakir MS, Supangat A: **Metal phthalocyanine: fullerene composite nanotubes via templating method for enhanced properties.** *Nanoscale Res Lett* 2015, **10**(1):1-8
48. Chatterjee K, Sarkar S, Jagajjanani Rao K, Paria S: **Core/shell nanoparticles in biomedical applications.** *Advances in Colloid and Interface Science* 2014, **209**(0):8-39.

49. Tchoulfian P, Donatini F, Levy F, Dussaigne A, Ferret P, Pernot J: **Direct Imaging of p–n Junction in Core–Shell GaN Wires.** *Nano letters* 2014, **14**(6):3491-3498
50. Wei LL, Hoong TC, Sulaiman K, Daik R, NM S: **Synthesis and Characterization of Solution Processable Organic Ultraviolet (UV) Photodetector based on 2,2'-Bithiophene End-Capped Dihexyloxy Phenylene Pentamer.** (will be published elsewhere)
51. Cullity BD: **Elements of X-ray diffraction.** 1978, Addison-Wesley, Philippines
52. Battaglia C, Hsu C-M, Söderström K, Escarré J, Haug F-J, Charrière M, Boccard M, Despeisse M, Alexander DTL, Cantoni M, Cui Y, Ballif C: **Light Trapping in Solar Cells: Can Periodic Beat Random?** *ACS Nano* 2012, **6**(3):2790-2797.
53. Sai H, Koida T, Matsui T, Yoshida I, Saito K, Kondo M: **Microcrystalline silicon solar cells with 10.5% efficiency realized by improved photon absorption via periodic textures and highly transparent conductive oxide.** *Applied Physics Express* 2013, **6**(10):104101.
54. Sai H, Kondo M, Saito K: **Periodic structures boost performance of thin-film solar cells.** <http://spie.org/x91297.xml>. Accessed 20 April 2015
55. Kietzke T: **Recent advances in organic solar cells.** *Advances in OptoElectronics* 2007, Article ID 40285.
56. Kumar B, Kim SW: **Energy harvesting based on semiconducting piezoelectric ZnO nanostructures.** *Nano Energy* 2012, **1**(3):342-355.
57. Liang D, Kang Y, Huo Y, Chen Y, Cui Y, Harris JS: **High-efficiency nanostructured window GaAs solar cells.** *Nano letters* 2013, **13**(10):4850-4856
58. Abdulrazzaq OA, Saini V, Bourdo S, Dervishi E, Biris AS: **Organic solar cells: a review of materials, limitations, and possibilities for improvement.** *Particulate Science and Technology* 2013, **31**(5):427-442.
59. Cates NC, Gysel R, Bailey Z, Miller CE, Toney MF, Heeney M, McCulloch I, McGehee MD: **Tuning the properties of polymer bulk heterojunction solar cells by adjusting fullerene size to control intercalation.** *Nano letters* 2009, **9**(12):4153-4157.
60. Hoppe H, Niggemann M, Winder C, Kraut J, Hiesgen R, Hinsch A, Meissner D, Sariciftci NS: **Nanoscale morphology of conjugated polymer/fullerene-based bulk-heterojunction solar cells.** *Advanced Functional Materials* 2004, **14**(10):1005-1011.
61. Bright WE, Decius JC, Paul CC: **Molecular vibrations: the theory of infrared and raman vibrational spectra.** 1955, McGraw-Hill Book Company, Inc.
62. Francis RD, William GF, Freeman FB: **Characteristic Raman frequencies of organic compounds.** 1973, John Wiley & Sons Inc.

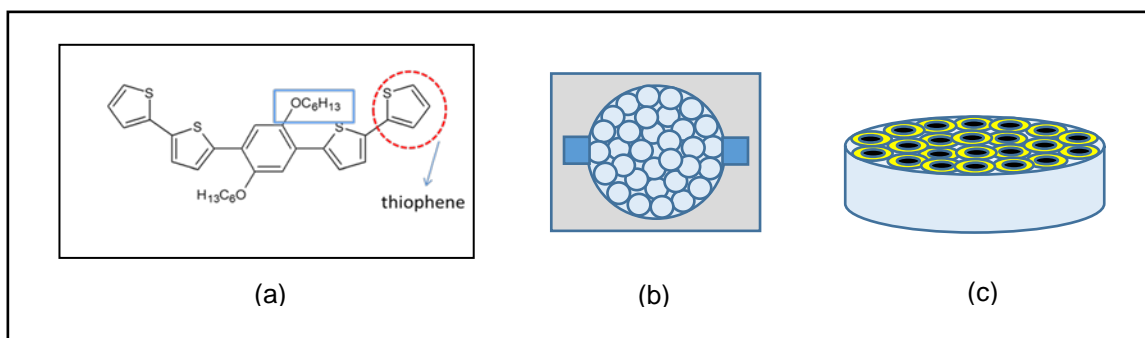


Figure 1 (a) Molecular structure of BHBT₂. (b) Illustration of porous alumina template being stuck on glass substrate. (c) Illustration of infiltrated BHBT₂.

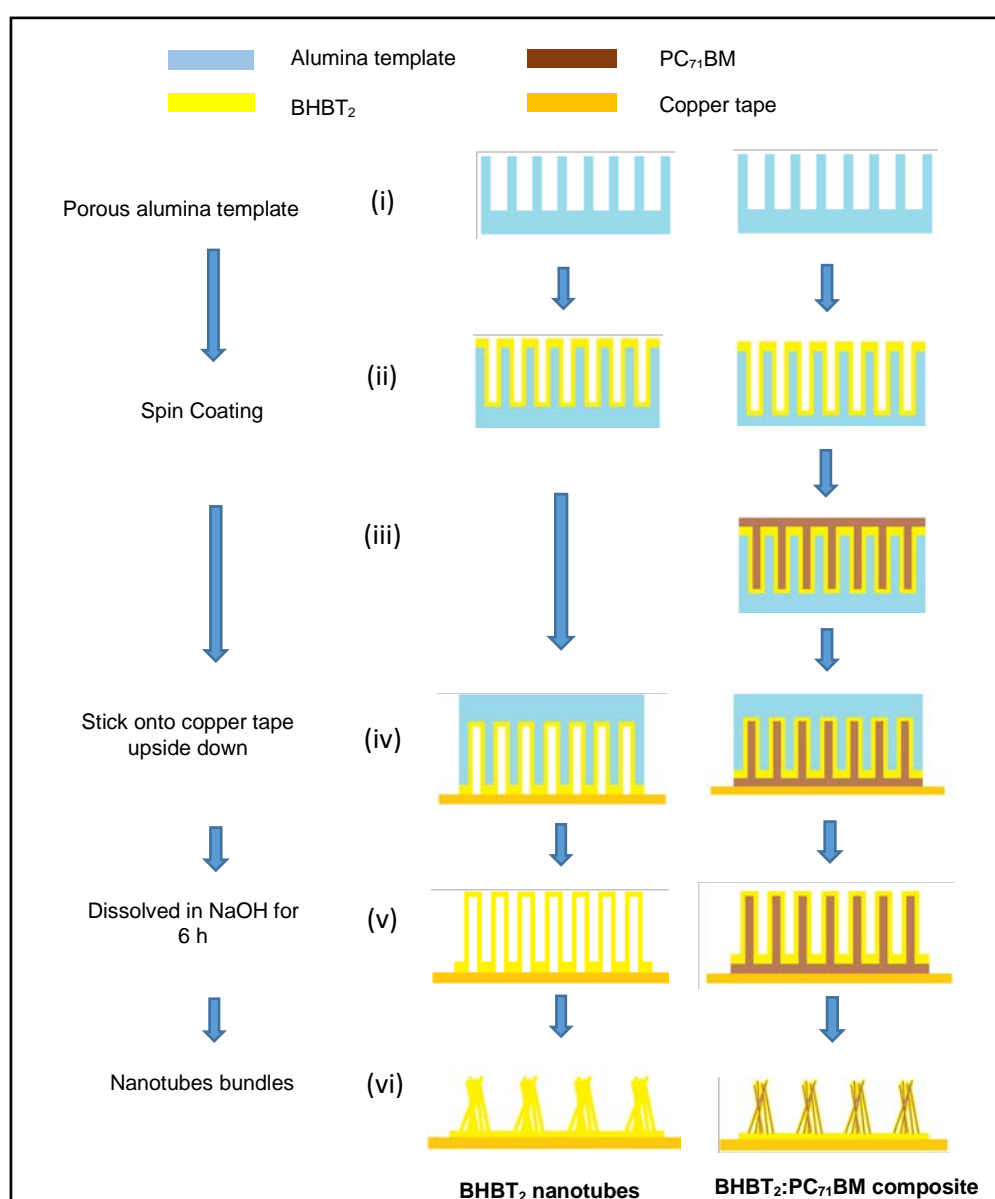


Figure 2 Schematic illustrations on the formation of BHBT₂ nanotubes and BHBT₂:PC₇₁BM composite nanotubes.

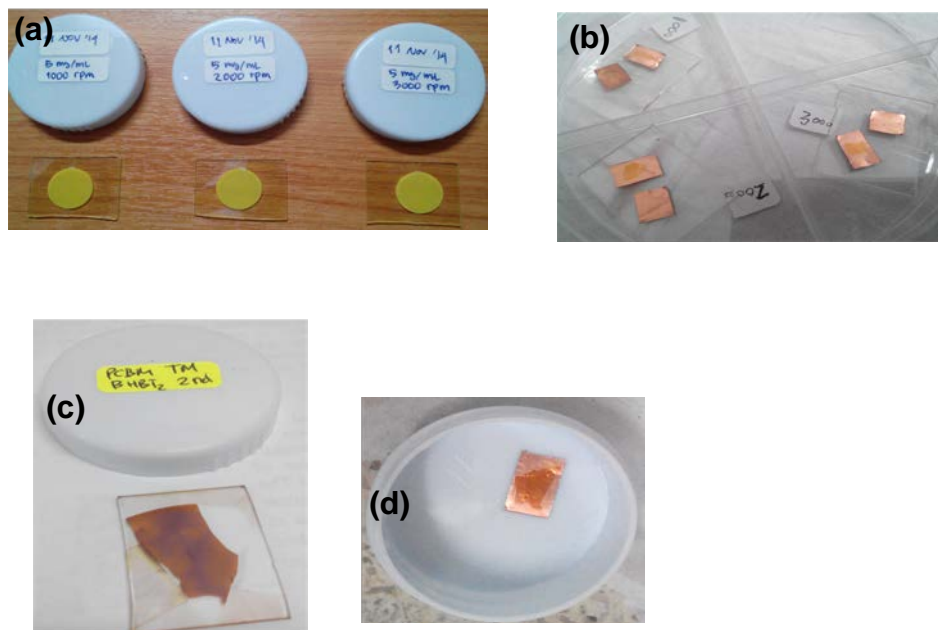


Figure 3 (a) Infiltrated BHBT₂ that spin coated at three different rates of 1000, 2000 and 3000 rpm. (b) BHBT₂ nanotubes stick upside down on copper tape. (c) BHBT₂:PC₇₁BM composite nanotubes before dissolution. (d) BHBT₂:PC₇₁BM composite nanotubes stick upside down on copper tape.

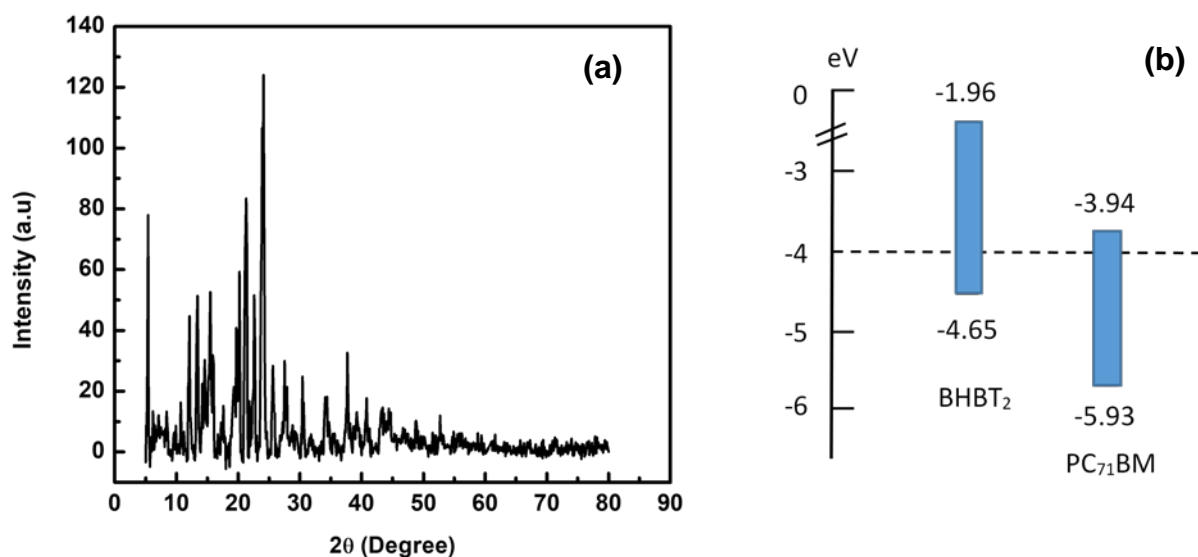


Figure 4 (a) XRD measurement of pristine BHBT₂. (b) Vacuum level (energy diagram) of BHBT₂ and PC₇₁BM.

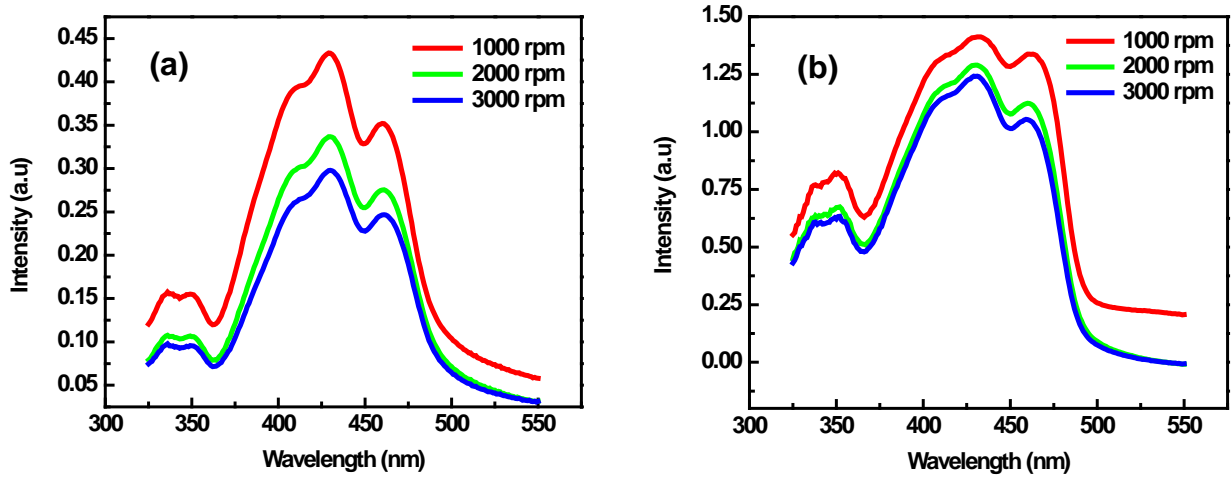


Figure 5 (a) UV-vis absorption spectra of BHBT₂ thin films. (b) UV-vis absorption spectra of BHBT₂ nanotubes.

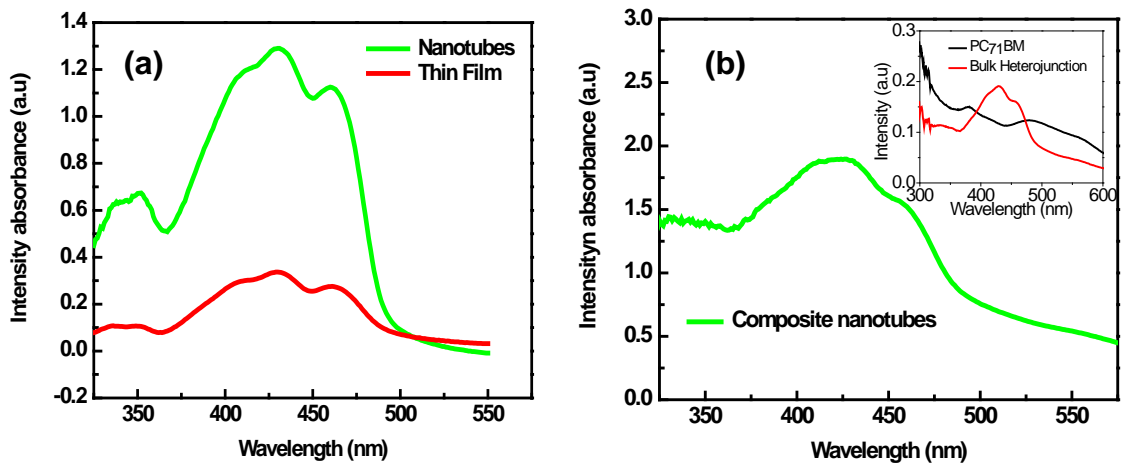


Figure 6 UV-vis absorption spectra of (a) BHBT₂ thin films and nanotubes (b) BHBT₂ composite nanotubes and BHBT₂ bulk heterojunction, PC₇₁BM thin films (inset).

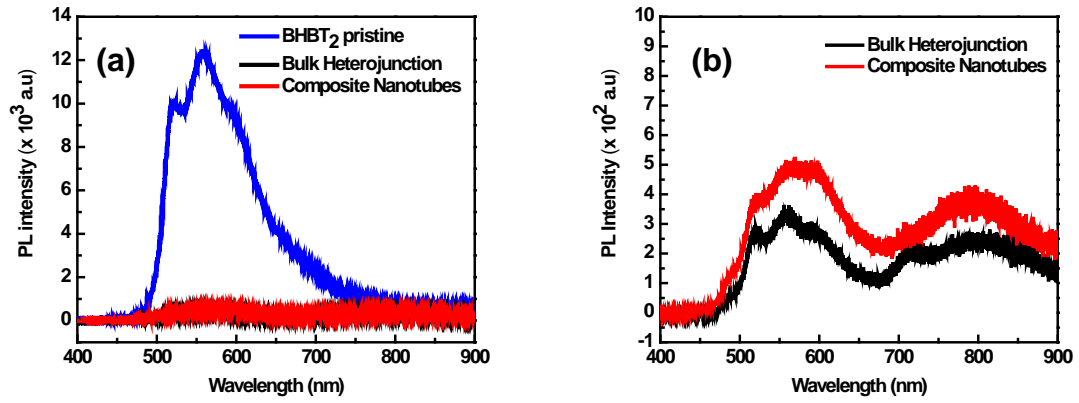


Figure 7 (a) Photoluminescence spectra of BHBT₂ thin films, bulk heterojunction and composite nanotubes. (b) Photoluminescence comparison spectra between BHBT₂ bulk heterojunction and composite nanotubes.

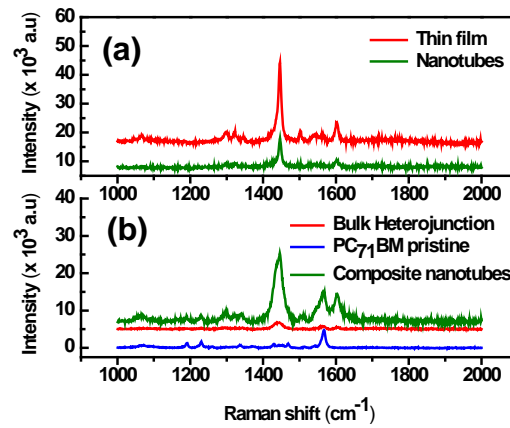


Figure 8 (a) Raman spectra of BHBT₂ thin films and composite nanotubes. (b) Raman spectra of BHBT₂ bulk heterojunction, composite nanotubes and PC₇₁BM.

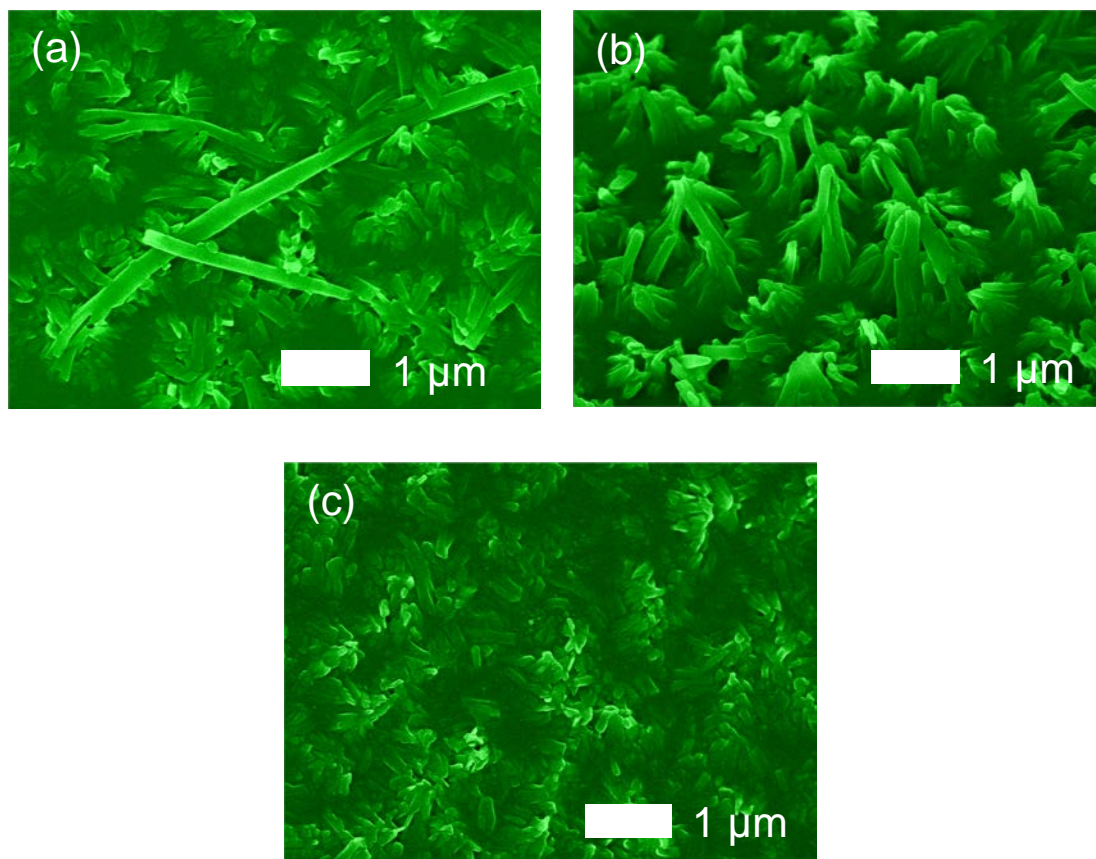


Figure 9 FESEM images of BHBT₂ nanotubes at spin coating rate of (a) 1000 rpm (b) 2000 rpm (c) 3000 rpm.

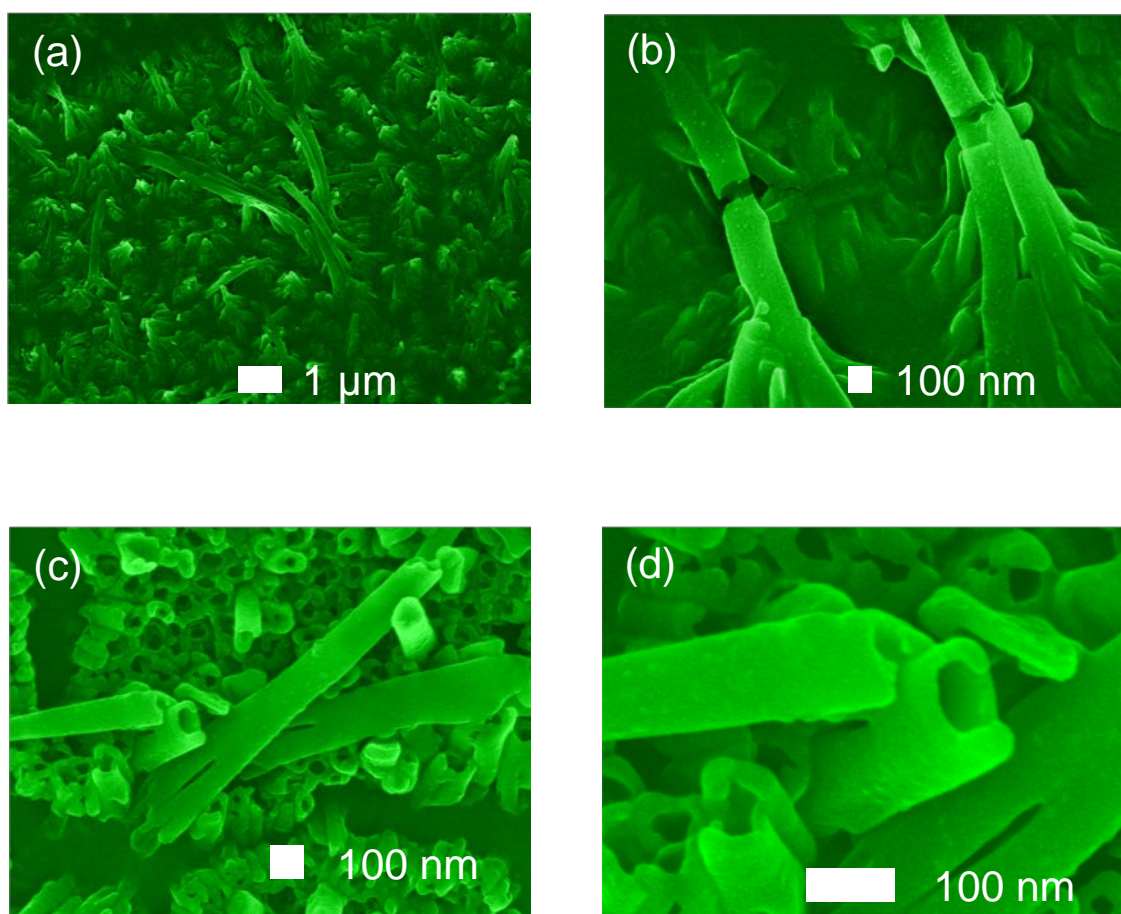


Figure 10 (a) and (b) FESEM images of BHBT₂ nanotubes spin-coated at 2000 rpm. (c) and (d) FESEM images of BHBT₂:PC₇₁BM composite nanotubes spin-coated at 2000 rpm.

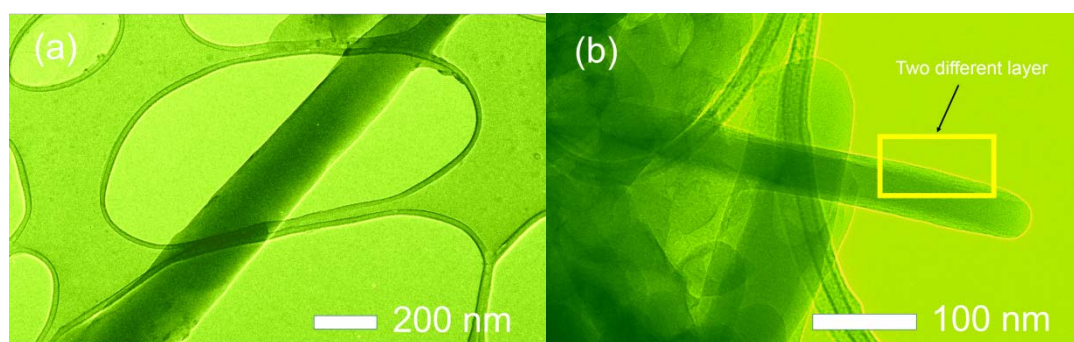


Figure 11 HRTEM images of (a) BHBT₂ nanotubes (b) BHBT₂:PC₇₁BM composite nanotubes.

Table 1 Raman peak positions of BHBT₂ and BHBT₂ : PC₇₁BM [62]

Raman Shift				
BHBT ₂		BHBT ₂ PC ₇₁ BM		
Thin Film (at 2000 rpm)	Nanotubes (at 2000 rpm)	Bulk heterojunction (at 2000 rpm)	Composites Nanotubes (at 2000 rpm)	Vibrational Assignments
1067	1068	1067	1068	C=S stretch Ethylene trithiocarbonate
-	-	1188	1189	Ring “breathing”
-	-	1227	1231	Ring vibration Para-disubstituted benzenes
1297	1299	1295	1299	CC bridge bond stretch
1324	1325	1328	1322	Ring vibration
1344	-	1342	1338	CH deformation
1445	1446	1443	1443	Ring stretch 2- Substituted thiophenes
1503	1503	1507	1505	Symmetric C=C stretch
1544	1544	-	-	C=C stretch
1566	1564	1565	1567	C=C stretch
1601	1602	1603	1604	C=C stretch